

1 **Changes of oscillatory and aperiodic neuronal activity in working memory**
2 **following anaesthesia: a prospective observational study**

3

4 Janna D. Lendner^{*1,2}, Ulrich Harler³, Jonathan Daume⁴, Andreas K. Engel⁴, Christian
5 Zöllner³, Till R. Schneider^{*4}, Marlene Fischer^{*3,5}

6

7 ¹ *Dept. of Anaesthesiology and Intensive Care Medicine, University Medical Centre Tübingen, 72076*
8 *Tübingen, Germany*

9 ² *Hertie Institute for Clinical Brain Research, 72076 Tübingen, Germany*

10 ³ *Dept. of Anaesthesiology, University Medical Centre Hamburg-Eppendorf, 20246 Hamburg, Germany*

11 ⁴ *Department of Neurophysiology and Pathophysiology, University Medical Center Hamburg-*
12 *Eppendorf, 20246 Hamburg, Germany*

13 ⁵*Department of Intensive Care Medicine, University Medical Centre Hamburg-Eppendorf, 20246*
14 *Hamburg, Germany*

15 * These authors contributed equally to this work

16

17 **Corresponding author**

18 Janna D. Lendner. Email: janna.lendner@med.uni-tuebingen.de

19

20 **Short title**

21 Neurophysiology of postoperative cognitive function

22

23 **Keywords**

24 Aperiodic activity, 1/f, spectral slope, EEG, neuropsychology, oscillations,
25 perioperative cognitive disorders, working memory, general anaesthesia

26 **Abstract**

27 **Background:** Anaesthesia and surgery can lead to cognitive decline, especially in the
28 elderly. However, to date, the neurophysiological underpinnings of perioperative
29 cognitive decline remain unknown.

30 **Methods:** We included male patients, who were 60 years or older scheduled for
31 elective radical prostatectomy under general anaesthesia. We obtained
32 neuropsychological (NP) tests as well as a visual match-to-sample working memory
33 (WM) task with concomitant 62-channel scalp electroencephalography (EEG) before
34 and after surgery.

35 **Results:** A total number of 26 patients completed neuropsychological assessments
36 and EEG pre- and postoperatively. Behavioural performance declined in the
37 neuropsychological assessment after anaesthesia (total recall; *t*-tests: $t_{25} = -3.25$,
38 Bonferroni-corrected $p = 0.015$ $d = -0.902$), while WM performance showed a
39 dissociation between match and mis-match accuracy (*rmANOVA*: match*session $F_{1,25}$
40 $= 3.866$, $p = 0.060$). Distinct EEG signatures tracked behavioural performance: Better
41 performance in the NP assessment was correlated with an increase of non-oscillatory
42 (aperiodic) activity, reflecting increased cortical activity (*cluster permutation tests*: total
43 recall $r = 0.66$, $p = 0.029$, learning slope $r = 0.66$, $p = 0.015$), while WM accuracy was
44 tracked by distinct temporally-structured oscillatory theta/alpha (7 – 9 Hz), low beta
45 (14 – 18 Hz) and high beta/gamma (34 – 38 Hz) activity (*cluster permutation tests*:
46 matches: $p < 0.001$, mis-matches: $p = 0.022$).

47 **Conclusions:** Oscillatory and non-oscillatory (aperiodic) activity in perioperative scalp
48 EEG recordings track distinct features of perioperative cognition. Aperiodic activity
49 provides a novel electrophysiological biomarker to identify patients at risk for
50 developing perioperative neurocognitive decline.

51 **Introduction**

52 Postoperative cognitive impairment after surgery and anaesthesia includes
53 postoperative delirium (POD)¹, delayed neurocognitive recovery (DNCR) and
54 postoperative neurocognitive disorders^{2, 3}, all of which are associated with increased
55 morbidity and mortality.¹⁻³ Elderly patients above 60 years are at high risk^{2, 4, 5} to suffer
56 from perioperative cognitive decline with incidences of up to 25 %.³ Several cognitive
57 domains such as attention, memory, and executive functions can be affected by
58 DNCR.⁶ Working memory (WM) maintenance is one function that may be affected
59 postoperatively even in the long term, which has been shown in both animal and
60 human studies.⁷⁻⁹ Neurophysiological studies in healthy human participants showed
61 specific patterns of oscillatory neuronal activity in several frequency bands during the
62 maintenance interval of WM tasks.¹⁰⁻¹³ Therefore, this study aimed at investigating the
63 changes of oscillatory activity before and after general anaesthesia for elective non-
64 cardiac surgery in a visual WM task.

65 In addition to changes in oscillatory neuronal activity after surgery, we examined
66 the modulation of aperiodic neuronal activity, which can be quantified by the spectral
67 slope of the $1/f^x$ exponential function of the power spectrum (PSD).¹⁴ Recent evidence
68 demonstrated that aperiodic activity contains rich information about the current
69 behavioural state. It is related to arousal in sleep and anaesthesia,¹⁵⁻¹⁸ but also
70 modulated during various cognitive tasks such as attention and working memory.^{18, 19}

71 To address these outstanding questions, we recorded both a cognitive
72 neuropsychological (NP) test battery, as well as a visual WM task with simultaneous
73 whole-head 62-channel scalp EEG before and after general anaesthesia in patients
74 undergoing radical prostatectomy to assess 1) perioperative cognitive performance
75 and 2) concomitant alterations of electrophysiological patterns. Specifically, we

76 hypothesized that anaesthesia alters oscillatory activity in the theta, alpha and beta
77 band, as these frequencies showed pronounced changes during WM maintenance.²⁰
78 In addition, we examined aperiodic activity, as measured by the spectral slope of the
79 power spectrum¹⁵⁻¹⁷, across pre- and postoperative sessions and investigated how
80 oscillatory and aperiodic electrophysiological signatures, relate to cognitive
81 performance.

82

83

84 **Material and Methods**

85

86 ***Ethics approval***

87 The study protocol was approved by the local ethics committee of the Hamburg
88 Chamber of Physicians (protocol number PV4782; 27.04.2016). All study participants
89 gave written informed consent before the initiation of study-related procedures.

90

91 ***Design, setting and participants***

92 This prospective observational study was performed at a high-volume prostate
93 cancer centre in Northern Germany. Between June 2016 and July 2017, we included
94 a convenience sample of patients aged 60 years or older, who spoke German fluently
95 and were scheduled for robot-assisted radical prostatectomy. Patients with pre-
96 existing cognitive impairment or cerebrovascular disease were excluded. Study
97 participants completed a neuropsychological (NP) assessment for cognitive function
98 and performed a WM task on the day before surgery *and* on one day post-surgery (2nd-
99 4th day). For details on data collection and anaesthesiologic management see
100 Supplementary Information.

101

102 ***Neuropsychological Assessment***

103 The NP test battery included the California Verbal Learning Test (CVLT), the
104 Trail Making Test (TMT), the Grooved Pegboard test (GPT) and the Digit Span
105 Forward Test (DS; **Fig. 1**). To obtain standardized test scores for each subtest of the
106 CVLT, we calculated the difference between pre- and postoperative scores for each
107 patient and divided the result by the baseline standard deviation (SD). For the TMT,
108 the GP and the DS z-scores were calculated accordingly after subtracting the practice

109 effect. A negative z-score for CVLT total recall, CVLT learning slope as well as the digit
110 span (and a positive z-score for TMT-B and DS) indicated a worse performance in the
111 second compared to the first session.

112

113 ***Working Memory Task***

114 For the assessment of task-related electrophysiologic changes, we chose a WM
115 task, since impairment in WM has been implicated in perioperative cognitive
116 disorders.^{21–23} Pre- and postoperative sessions consisted of two conditions – a visual
117 delayed match-to-sample task (memory condition) as well as a non-mnemonic visual
118 discrimination task (control condition) as described previously.²⁰ Stimuli were black
119 and white line drawings of natural objects (**Fig. 1**).²⁴ In a total of 8 blocks (4 of each
120 memory and control) with 52 trials each, patients completed 416 trials (208 of each
121 condition) consisting of unique sample/probe pairs (task details see Supplemental
122 Information).²⁰

123

124 ***Behavioural data analysis***

125 Reaction time (RT in seconds) and accuracy (AC between 0 and 1, where 1
126 equals 100%) were determined for every condition and session (session 1 – before,
127 session 2 – after anaesthesia; condition – memory or control). Memory performance
128 was further split into match (RT_{Match}/AC_{Match}) and non-match trials ($RT_{Non-Match}/AC_{Non-}$
129 $Match$) and then averaged across trials. Performance differences between matches and
130 non-matches were calculated by subtracting the second from the first session.

131

132

133 ***Electroencephalography***

134 EEG data was recorded during the working memory and the control task from
135 an equidistant 62 electrode scalp montage montage (Easycap, Herrsching, Germany)
136 with two additional electrooculography (EOG) channels below the eyes and referenced
137 against the tip of the nose. EEG was recorded with a passband of 0.016-250 Hz and
138 stored with a sampling rate of 1000 Hz using BrainAmp amplifiers (BrainProducts,
139 Gilching, Germany) in a dimly lit, sound-attenuated recording room.

140

141 ***Electrophysiological data analysis***

142 Data analysis was performed using Matlab R2018b (The MathWorks, Inc.,
143 Natick, Massachusetts, United States) and the FieldTrip²⁵ toolbox (version 20172908)
144 as well as custom code. For pre-processing, electrophysiological data was notch-
145 filtered to remove line noise in 0.1 Hz steps (bandstop filter; 49 to 51 and 99 to 101
146 Hz) as well as high- (0.1 Hz) and lowpass-filtered (100 Hz). Data was then averaged
147 using a common median reference excluding the two EOG channels.
148 Electrophysiological data was epoched into 5-second segments time-locked to sample
149 onset (-1 to +4 s).

150 Trials containing jumps or strong artifacts were detected using FieldTrip²⁵
151 (ft_rejectvisual) and rejected after visual inspection. Next, independent component
152 analysis (fastica²⁶) was used to remove eye-blinks, horizontal eye-movements,
153 electrocardiogram artifacts or broadband noise based on the component spectrum,
154 topography and time course.

155

156

157 ***Spectral power analysis***

158 Time-frequency decomposition was performed on epoched data using a sliding
159 window Fast Fourier Transformation (*mtmconvo*²⁵) between -0.5 to 3.5 seconds in 50
160 ms steps and in the frequency range from 1 to 40 Hz in 1 Hz steps using a 500 ms
161 Hanning taper with 50 % overlap. Each trial was then z-scored to a bootstrapped
162 baseline (-500 to 0 ms) using a permutation approach (pooled baseline of all trials per
163 channel; 1000 iterations).

164

165 ***Spectral slope analysis***

166 Calculation of spectral slope was performed on the PSD (settings see above)
167 between 30 to 40 Hz, in line with recent work.¹⁵ For each channel and trial, we obtained
168 a first-degree polynomial fit to the power spectra in *log-log* space (*polyfit.m*, MATLAB
169 and Curve Fitting Toolbox Release R2018b, The MathWorks, Inc., Natick,
170 Massachusetts, United States).

171

172 ***Statistical analysis***

173 For statistical comparison of behavioural data, we employed dependent
174 samples t-tests. All significant results were Bonferroni-corrected for multiple
175 comparisons, if not stated otherwise. Effect size was calculated using Cohen's d. To
176 determine the influence of conditions, sessions and trials type on behaviour, we utilized
177 Greenhouse-Geisser corrected 2-way repeated measures analysis of variance (RM-
178 ANOVA). To assess the spatial extent of the observed effects in EEG, we calculated
179 cluster-based permutation tests to correct for multiple comparisons as implemented in
180 FieldTrip²⁵ (Monte-Carlo method; maxsum criterion; 1000 iterations) reporting p- as
181 well as the sum of t-values. A permutation distribution was obtained by randomly

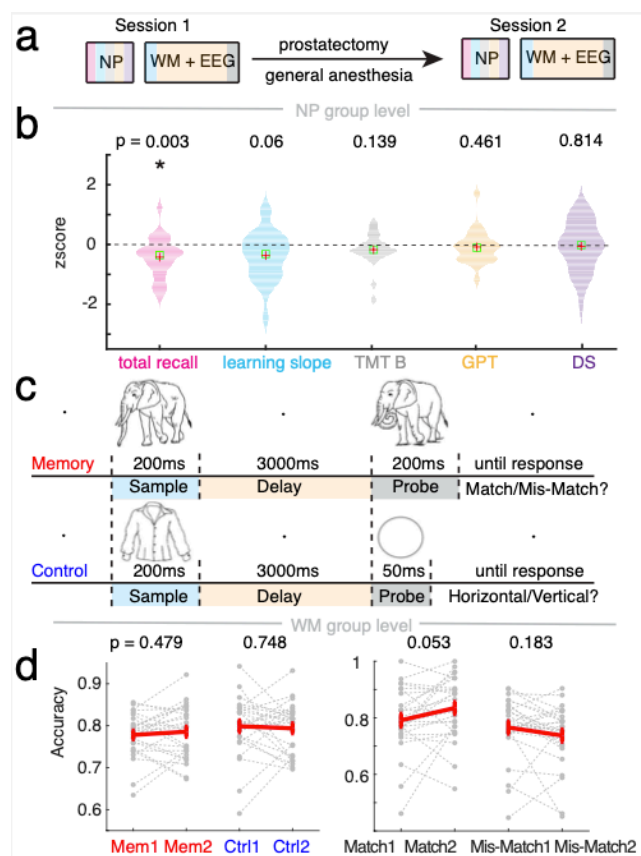
182 shuffling condition labels. Spatial clusters are formed by thresholding dependent
183 samples t-tests between control and memory as well as memory between sessions at
184 a p-value < 0.05 for the comparisons of ERP (**Fig. S5**), power (**Fig. 3**) and spectral
185 slope (5000 iterations; **Fig. 5**). To assess the spatial extent of a correlation between
186 WM/NP behaviour and power/slope differences between memory sessions in the delay
187 period (0.3 to 3.1 s; **Fig. 4, 5**), we used rank correlations at a p-value of < 0.05 for the
188 cluster test. To control for an influence of WM behaviour on the NP-slope association,
189 we utilized a partial correlation that partialled accuracy out before computing the
190 correlation. The results of this analysis should be regarded as hypothesis generating.

191

192

193 **Results**

194 A total of 41 male patients (for patient characteristics see **Table 1, S2**) were
 195 included in this study (flow chart see **Fig. S1**). Data analysis focused on 26 patients
 196 that completed both neuropsychology (NP) and working memory (WM) sessions pre-
 197 and post-operation, of whom seven fulfilled definition of DNCR (26.92 %).
 198 Demographic and clinical data of study participants including, who did not complete
 199 the postoperative assessments, are presented in Table S2.



200

201 **Figure 1: Cognitive performance before and after general anaesthesia.**

202 **a**, Study design: Neuropsychological (NP) tests and working memory (WM) task with
 203 electroencephalography (EEG) were obtained before (Session 1) and after (Session 2) prostatectomy
 204 under general anaesthesia.

205 **b**, NP test scores (n = 26). Only California Verbal Learning Task total recall (pink) showed significant
 206 changes compared to zero (p-value corrected for multiple comparisons = 0.015; * p < 0.05), revealing
 207 that patients could remember less words. TMT-B (grey): Trail Making Test B, GPT (orange): Grooved
 208 Pegboard Test, DS (purple): Digit Span. Red cross: mean. Green box: standard error of the mean
 209 (SEM).

210 **c**, Task design WM: Sample presentation (blue) is followed by 3 second delay (orange), then probe
 211 presentation (grey): in memory either exactly the same (match) or an altered version (non-match), in
 212 control, either a horizontally or vertically oriented ellipse (grey).

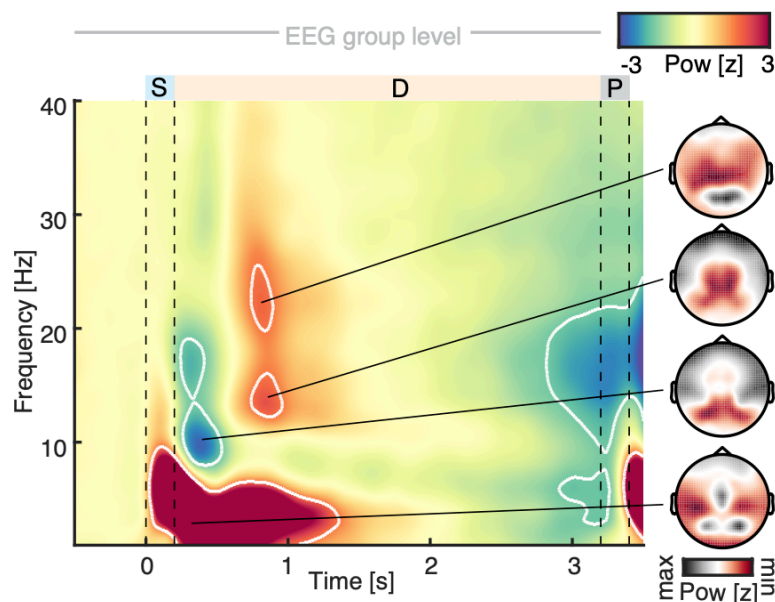
213 **d**, Accuracy of memory and control (left) and match and mis-match memory trials (right; n = 26).
 214 Discrimination of matches was more accurate after anaesthesia while less mis-matches were identified
 215 (t-test, p-values uncorrected). Grey dotted lines: single subjects. Red lines: mean +/- SEM.

216

217 *Cognitive performance before and after general anaesthesia*

218 Patients remembered less words in the post-anaesthesia NP session (CVLT
219 total recall/zero $t_{25} = -3.25$, Bonferroni-corrected $p = 0.015$ $d = -0.902$; **Fig. 1b, Table**
220 **S2**). In addition, they tended towards being slower in learning new words (CVLT
221 learning slope/zero $t_{25} = -1.97$, Bonferroni-corrected $p = 0.3$, $d = -0.546$). The other
222 NP tests did not differ between sessions (**Table S2, Fig. 1b**). Thus, subsequent
223 analysis focused on CVLT metrics.

224



225

226 **Figure 2: Grand average spectral power across all conditions and sessions.**

227 Left – temporal evolution. Cold colours - decrease, warm colours - increase compared to baseline (-0.5
228 to 0 s). White Contour marks a z-score of 1.65 (equivalent to $p < 0.05$, one-tailed). Note the low
229 frequency power increase (0-7 Hz) starts from stimulus presentation, in line with an ERP effect. In the
230 delay period (0.3 to 3.1 s), an alpha/beta (7-19 Hz) power decrease as well as a low beta (14-18 Hz)
231 and high beta (18-25 Hz) power increase emerge. Right – spatial extent of power changes (black –
232 maximal, red – minimal z-scored power). Note, the localization of alpha/beta effects to visual cortex and
233 of beta effect to parietal and motor cortices.

234

235 Between the two memory sessions of the WM task, overall accuracy was
236 comparable (values see **Table 2** and **Fig. 1**; *repeated-measures ANOVA*: condition
237 $F_{1,25} = 4.574$, $p = 0.042$; session $F_{1,25} = 0.012$, $p = 0.912$; condition*session $F_{1,25} =$

238 1.404, $p = 0.247$; *dprime t-test*: $p = 0.245$). When analysing match and mis-match trials
239 separately, there was an overall tendency for patients to become more accurate in
240 detecting matches and less so in recognizing mis-matches (**Fig. 1**; *repeated-measures*
241 *ANOVA*: match $F_{1,25} = 3.412$, $p = 0.077$; session $F_{1,25} = 0.497$, $p = 0.487$;
242 match*session $F_{1,25} = 3.866$, $p = 0.060$), in line with a response bias shift towards
243 matches (**Table 2**; *t-test*: $p = 0.049$). For reaction times, there were no overall, match
244 or mis-match differences (**Table 2**, **Fig. S2**), therefore, we focused on accuracy
245 differences between match and mis-match trials for subsequent analysis of any
246 association between WM behaviour and electrophysiology.

247 Interestingly, there was no relationship between accuracy and NP assessment
248 scores ($\Delta = Se2 - Se1$; $\Delta AC_{match}/z\text{-score total recall } r = 0.17$, $p = 0.417$; Δ
249 $AC_{match}/z\text{-score learning slope } r = 0.26$, $p = 0.191$; $\Delta AC_{mis\text{-}match}/z\text{-score total}$
250 $recall r = 0.05$, $p = 0.817$; $\Delta AC_{mis\text{-}match}/z\text{-score learning slope } r = -0.07$, $p = 0.724$;
251 **Fig. S2a**) indicating that they reflect different cognitive processes.

252

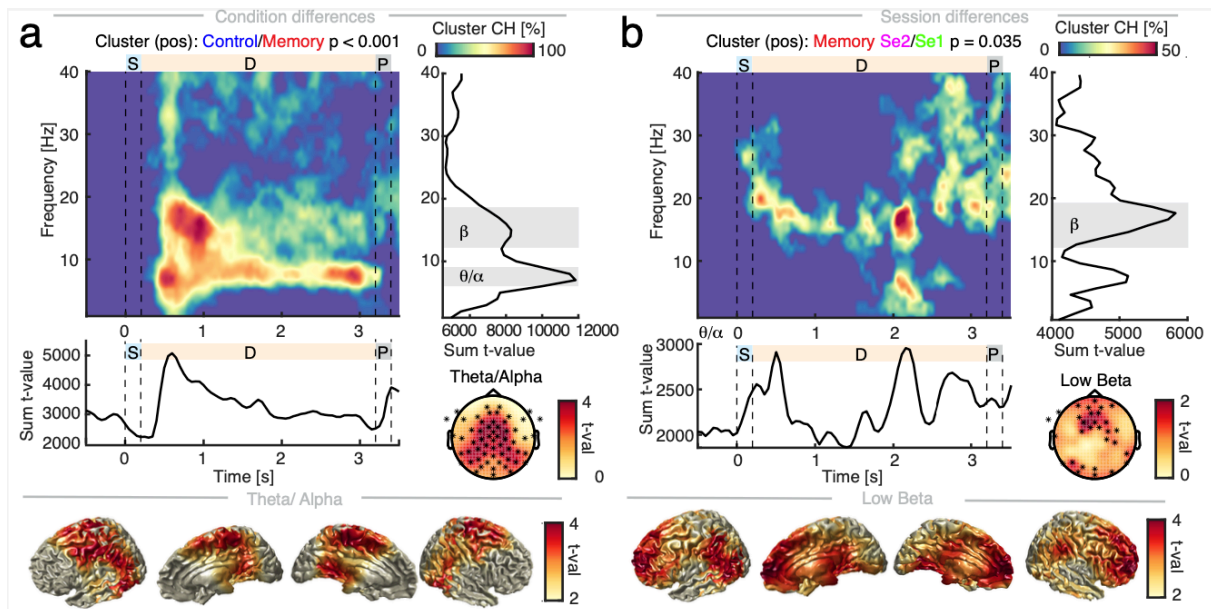
253 *Oscillatory activity in the beta frequency band is associated with a visual accuracy*

254 Grand average power (**Fig. 2**) across all subjects, conditions and sessions
255 revealed an early increase of delta/theta power (0.5 – 7 Hz), followed by a decrease in
256 the alpha/beta range (8 – 19 Hz) and an increment in the low and high beta frequency
257 band (12 – 16, 20 – 26 Hz) compared to baseline (-0.5 – 0 s), in line with recent work²⁰.
258 Here, we focused on these frequency bands and the delay period (0.3 – 3.1 s) where
259 stimulus related activity was absent.

260 Between conditions, we found that spectral power was significantly higher in the
261 control conditions (*cluster-based permutation t-test*: $t_{sum} = 6.53 \cdot 10^4$, $p < 0.001$) in the
262 theta/alpha (7 – 9 Hz) and low beta band (14 – 18 Hz), revealing a sustained

263 suppression of theta/alpha power in the memory conditions (**Fig. 3a**, single sessions
 264 see **Figures S4**).

265



266

267 **Figure 3: Spectral power changes across conditions and sessions.**

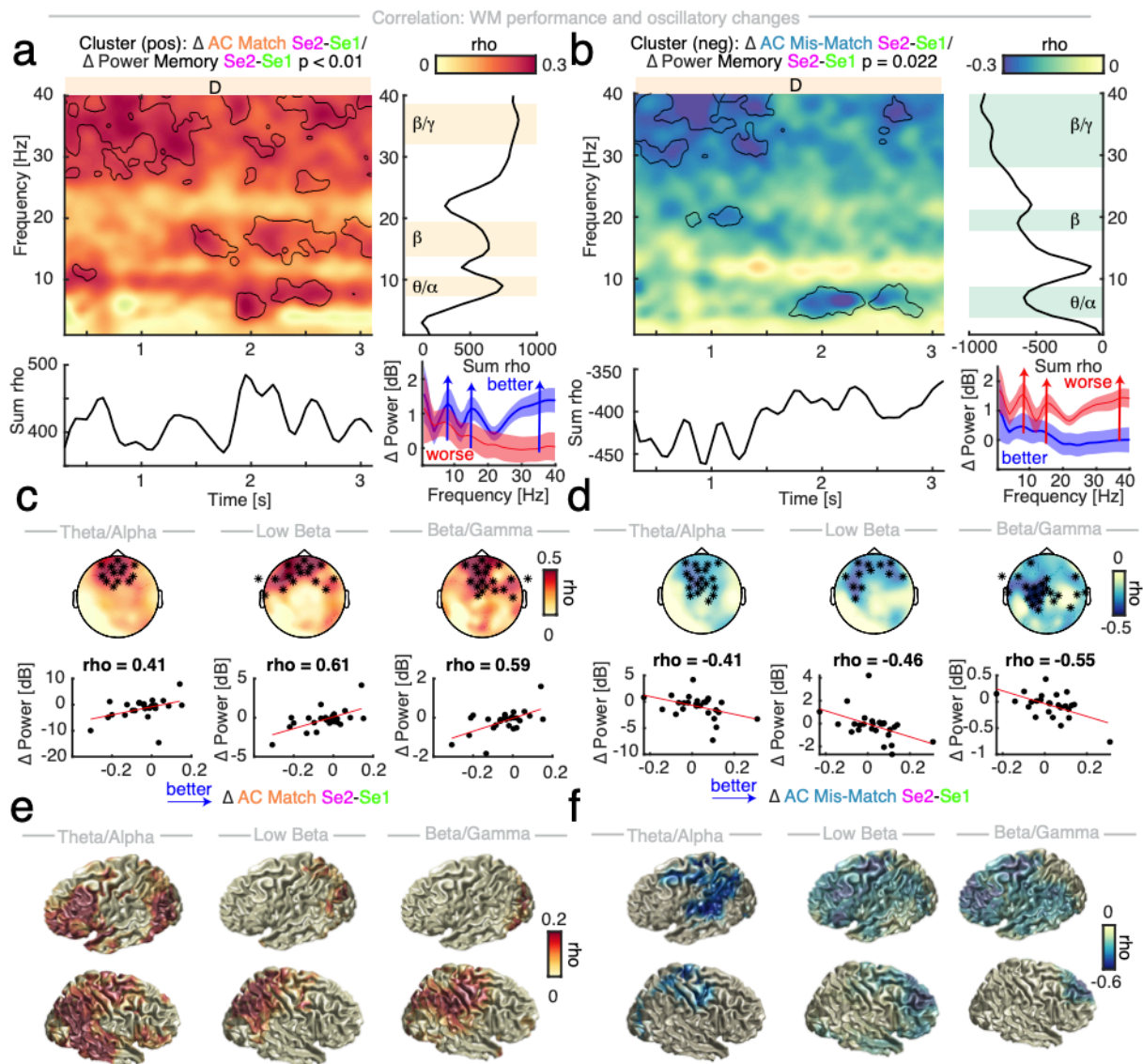
268 Sequence of WM task: blue/S – sample, orange/D – delay, grey/P – probe. **a**, Left upper – Condition
 269 power differences between control and memory averaged across sessions (baseline-corrected; $n = 26$).
 270 Colour: percent of channels in cluster from blue – 0 to red – 100%. Right upper – Sum of t-values per
 271 frequency. Note the peaks in theta/alpha (7 – 9 Hz) and low beta (14 – 18 Hz). Left middle – Sum of t-
 272 values per time. Note the increased activity in theta/alpha in the control condition compared to the
 273 memory one, revealing a sustained suppression in memory trials. Right middle – spatial extent of
 274 theta/alpha power differences on scalp. Lower panel – source-interpolated on a template brain in MNI
 275 space. Low beta power exhibited a similar spatial spread and was therefore omitted here. Colour-coded:
 276 yellow – no difference to red – strong difference.

277 **b**, Left upper – Memory session power differences (baseline-corrected; $n = 26$). Colour-coded: percent
 278 of channels in cluster from blue – 0 to red – 50%. Right upper – Sum of t-values per frequency. Note
 279 the peak in low beta (14 – 18 Hz). Left middle – Sum of t-values per time. Note the pulsing of beta during
 280 delay. Right middle – spatial extent of low beta power differences on scalp. Lower panel – source-
 281 interpolated on template brain in MNI space. Colour-coded: yellow – no difference to red – strong
 282 difference.

283

284 Between memory sessions (**Fig. 3b**), power significantly increased post-
 285 anaesthesia (*cluster-based permutation t-test*: $t_{\text{sum}} = 2.16 \cdot 10^4$, $p = 0.035$) in the low
 286 beta band (14 – 18 Hz). There were no differences between control sessions (*cluster-
 287 based permutation t-test*: $p = 0.401$). Importantly, this effect could not be explained by
 288 ERP differences (**Fig. S5**). The power increase in the low beta frequency band as well
 289 as in the theta/alpha and high beta/low gamma ranges were significantly correlated

290 with a better accuracy in detecting match trials (**Fig. 4a**; *cluster-based permutation*
 291 *correlation*: $t_{\text{sum}} = 5.89 \cdot 10^4$, $p < 0.001$) but with a worse performance in recognizing
 292 mis-matches (**Fig. 4b**; *cluster-based permutation correlation*: $t_{\text{sum}} = -3.85 \cdot 10^4$, $p =$
 293 0.022). Note, that power changes in these frequency bands were not correlated with
 294 the NP scores (**Fig. S3c,e**, *cluster-based permutation correlation with power session*
 295 *difference*: total recall $p = 0.439$, learning slope $p = 0.358$).
 296



297
 298

299 **Figure 4: Behaviourally relevant oscillatory spectral changes.**
 300 Association between memory session spectral power (Δ Se2 – Se1) and accuracy (AC) differences in
 301 the delay (0.3 to 3.1 s, $n = 26$). **a**, Match: Left upper – cluster permutation correlation. Black contour –
 302 $\rho > 0.2$. Orange/D – delay. Right upper – Sum of t-values per frequency. Note the peaks in theta/alpha
 303 and low beta frequency range as well as a broadband effect with a peak in the high beta/low gamma
 304 range. Lower left – Sum of t-values over time. Lower right – Median AC Match split of power difference
 305 (Δ Se2 – Se1; baseline-corrected; mean with SEM). Red – worse, blue – better performance. **b**, Mis-

306 Match: Left upper – cluster permutation correlation. Black contour – $\rho < -0.2$. Orange/D – delay. Right
307 upper – Sum of t-values per frequency. Note the negative peaks in similar frequency ranges. Lower left
308 – Sum of t-values over time. Lower right – Median split AC Mis-match of power difference ($\Delta Se_2 - Se_1$;
309 baseline-corrected; mean with SEM). Red – worse, blue – better performance. Correlation of AC and
310 power in the theta/alpha (7 – 9 Hz), low beta (14 – 18 Hz) and high beta/low gamma range (34 – 38 Hz).
311 **c**, AC Match: Upper row – Spatial extent, Lower row – correlation ρ . **d**, AC Mis-match: Upper row –
312 Spatial extent, Lower row – correlation ρ . **e**, AC Match: Rho-values source-interpolated on a standard
313 template brain in MNI space (threshold $p < 0.05$). **f**, AC Mis-match: Rho-values in MNI space.
314

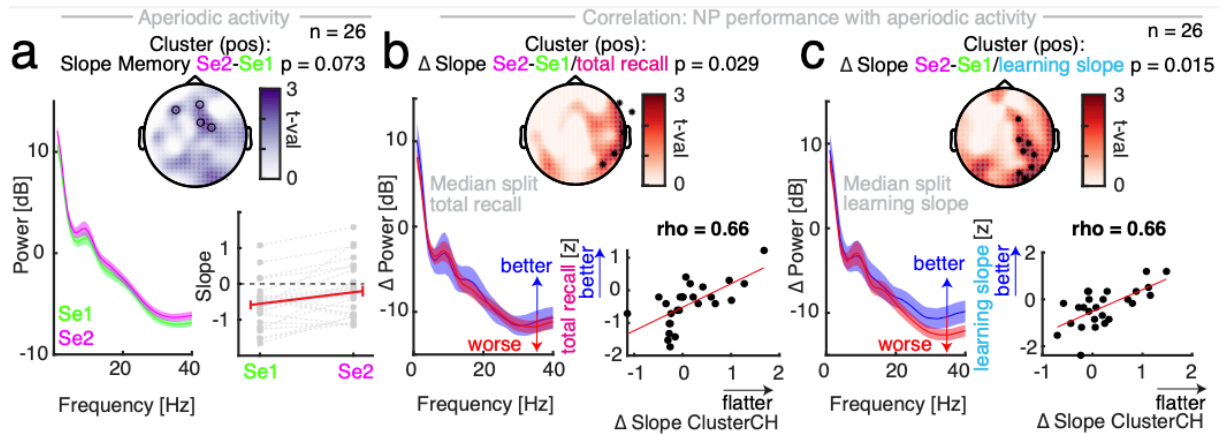
315 *Increased aperiodic activity is associated with better performance in*
316 *neuropsychological assessment*

317 In line with an increase of aperiodic activity, the PSD became flatter (i.e. the
318 slope decreased) in the post-anaesthesia memory session (**Table 2, Fig. 5a**; *cluster-*
319 *based permutation t-test*: $t_{sum} = 9.60$, $p = 0.073$).

320 A flattening of the PSD was associated with a better performance in the NP
321 CVLT total recall (**Fig. 5b-c**; *cluster-based permutation correlation*: Δ slope/z-score
322 total recall $r = 0.66$, $p = 0.029$) and learning slope (*cluster-based permutation*
323 *correlation*: Δ slope/z-score learning slope $r = 0.66$, $p = 0.015$) but not with the WM
324 performance (**Fig. S3f**; *post-hoc correlations*: Δ slope of cluster channels/ Δ AC match
325 $r = 0.19$, $p = 0.365$; Δ slope of cluster channels/ Δ AC mis-match $r = 0.03$, $p = 0.876$).
326 Beta power increases were not associated with slope decreases (14 – 18 Hz; *post-hoc*
327 *correlation*: $r = 0.15$, $p = 0.449$; **Fig. S3d**).

328

329



330

331

332

Figure 5: Aperiodic activity in pre- and post-anaesthesia memory sessions.

333

a, Lower left – Spectral power. Middle – Spectral slope session difference borders on significance (*cluster permutation t-test* $t_{25} = 9.6$, $p = 0.073$) with a focus on frontal channels (black circles). Lower right – Spectral slopes (*post-hoc t-test*: $t_{25} = 1.97$, $p = 0.060$, $d = 0.31$). Grey dotted lines – single subjects. Red line – mean \pm SEM.

336

Association between session differences (Δ Se2 – Se1) of spectral slope and neuropsychological test scores (negative z-scores indicate worse performance; $n = 26$). **b**, Lower left – Median split of spectral power difference by total recall z-scores. Blue – better, red – worse performance. Middle - Spatial extent of and right lower – correlation between Δ slope with z-score total recall in cluster channels. **c**, Lower left – Median split of spectral power difference by learning slope z-scores. Blue – better, red – worse performance. Middle - Spatial extent of and right lower – correlation between Δ slope and z-score of learning slope in cluster channels.

344

345

346 **Discussion**

347 The current study examined the impact of surgery and general anaesthesia on
348 postoperative cognitive performance and electrophysiology using neuropsychological
349 (NP) assessment and a visual working memory (WM) task with concomitant scalp
350 EEG. We observed a striking double dissociation between cognitive performance and
351 EEG signatures. Behavioural results revealed that patients' working memory
352 performance in general did not change despite surgery under general anaesthesia.²⁷⁻
353 ²⁹ However, performance differences between match and mis-match trials emerged in
354 the postoperative session. Performance increases in match trials in the WM task were
355 associated with an enhancement of low and high beta oscillations in the postoperative
356 session. Additionally, better cognitive function in NP assessment was accompanied by
357 a rise of aperiodic, non-oscillatory brain activity. These findings reveal that rhythmic
358 and arrhythmic neural activity tracks distinct facets of peri-anaesthesia cognition.

359

360 ***Oscillatory signatures of working memory***

361 Neural oscillations in various frequency bands have been implicated in WM.¹³
362 While theta (3-8 Hz) oscillations have been related to successful recognition³⁰ and are
363 thought to temporally structure WM items¹³, alpha oscillations (8-12 Hz) are often
364 associated with inhibition^{31, 32} and assumed to suppress task-irrelevant activity.¹³ Beta
365 activity (13-30 Hz) reflects at least two functionally and spatially distinct components,
366 the sensorimotor beta oscillation that mediates motor control and frontal beta activity,
367 which is related to top-down cognitive processing.^{27, 28} Increased beta and gamma
368 activity (~40 Hz)¹⁰ have been linked to the active maintenance of information in WM.¹³
369 ^{20, 28} Here, we found a memory-related suppression of theta/alpha and low beta activity

370 (7-18 Hz; **Fig. 3a**) over fronto-parietal cortices in line with a release from inhibition in
371 task-relevant areas.^{31, 33}

372 Between pre- and post-anaesthesia memory sessions, low beta (14 – 18 Hz)
373 oscillations increased, occurring in bursts over frontal cortex during the entire delay
374 period (**Fig. 3b**) potentially signalling top-down control.^{27–29} Importantly, this beta
375 enhancement was associated with differential processing of match and non-match
376 trials in the WM task (**Fig. 4**). Increases in performance in match trials from pre- to
377 postoperative assessments were associated with increases in theta (7-9 Hz), low beta
378 (14-18 Hz), and beta/gamma (34-38 Hz) oscillatory activity. Whereas decreases in
379 performance in non-match trials from pre- to postoperative assessments were
380 associated with increases in theta (7-9 Hz) and beta/gamma (34-38 Hz) oscillatory
381 activity (**Fig.4**). Beta and gamma bursts during WM maintenance were suggested to
382 be related to readout and control mechanism in WM tasks³⁴ and also with inhibition of
383 competing visual memories.³⁵ Thus, our findings are well in line with theories proposing
384 that enhanced oscillatory synchrony enables the efficient network communication
385 which is the fundament of optimal cognitive processing.³⁶

386

387 ***The importance of aperiodic activity for cognitive function***

388 While some recent evidence suggests that a shift of oscillatory peak frequency
389 of the posterior alpha frequency activity can outlast anaesthesia and might relate to
390 cognitive performance³⁷, the importance of aperiodic activity for cognitive function in a
391 perioperative setting has not yet been investigated. Recently, several lines of inquiry
392 highlighted that aperiodic activity tracks task-related neural activity in a variety of
393 cognitive domains such as attention¹⁸, motor execution³⁸ and working memory^{14, 39} and
394 is related to better task performance. In the present study, we observed a similar

395 pattern, namely that enhanced aperiodic activity (i.e. flattening of the PSD/ decrease
396 of spectral slope) after anaesthesia was associated with a better performance in the
397 neuropsychological assessment (**Fig. 5**). If aperiodic activity was not enhanced or even
398 reduced after anaesthesia, patients performed worse (**Fig. 5**). Our findings
399 demonstrate that an increase of aperiodic activity tracks a selective activation of task-
400 relevant cortices resulting in better cognitive performance.

401

402 ***Anaesthetic-induced inhibition overhang as a potential contributor to***
403 ***postoperative neurocognitive impairment***

404 Experimental evidence and computational modelling have linked aperiodic
405 activity to the excitation to inhibition balance of the underlying neuronal population,
406 where an increase of inhibition (e.g. by GABAergic drugs like propofol) results in a
407 steepening of the PSD (i.e. an increase of spectral slope).¹⁵⁻¹⁷ Increased cortical
408 (excitatory) activity, on the other hand, led to a flattening of the PSD (i.e. a decrease
409 in slope) that was associated with improved task performance.^{18, 19} Computational
410 modelling established that aperiodic activity indexes the underlying balance between
411 excitatory and inhibitory neuronal activity on the population level¹⁷. Anaesthetics like
412 propofol and sevoflurane increase cortical inhibition via GABA receptors. Recent
413 electrophysiological studies confirmed that increased inhibition reduces aperiodic
414 activity as indexed by a steepening of the PSD, i.e. an increase of spectral slope.¹⁵⁻¹⁸

415 To date it remains unclear how fast this inhibition dissipates after drug
416 administration is discontinued. While the healthy young brain is resilient to
417 electrophysiological disturbances by anaesthesia⁴⁰, elderly patients are more sensitive
418 to anaesthetics and therefore more likely to enter burst suppression⁴ - a pattern of
419 brain activity induced by a maximum of inhibition where bursts of activity are followed

420 by periods of neuronal silence.⁴¹ Time spent in that (too) deep plane of anaesthesia is
421 an independent risk factor for developing POD.^{2, 42} Not only age but also individual
422 brain vulnerability plays a role in susceptibility to adverse cognitive outcomes after
423 anaesthesia: Patients that reacted with intraoperative EEG suppression at lower doses
424 of anaesthetics were more likely to develop POD.^{43, 44} In addition, a recent study that
425 examined EEG parameters before, during and after anaesthesia found that a lower
426 preoperative spectral edge frequency and gamma power were independently related
427 to the development of POD.⁵ Note that these findings could also be explained by a
428 steeper slope of the preoperative PSD (i.e. more inhibition) in the POD group
429 compared to the patients that did not develop POD. In the current study, patients that
430 showed an increase of aperiodic activity (less inhibition) after anaesthesia, performed
431 better in postoperative neuropsychological assessment whereas patients that
432 exhibited a decrease (more inhibition) performed worse (**Fig. 5**).

433 Taken together, these findings suggest that anaesthesia-induced inhibition
434 potentially outlasts drug administration in elderly patients and that this inhibition
435 overhang impedes optimal postoperative cognition. Pre-existing alterations of neuronal
436 balance between excitation and inhibition (such as a premedication with e.g.
437 benzodiazepines) could be a predisposing factor for developing postoperative
438 cognitive decline. Thus, aperiodic brain activity might provide a valuable marker to
439 track perioperative cognition - before, during and after anaesthesia.

440

441

442 ***Strengths and limitations***

443 Key advantages of the current study are: 1) It focused on electrophysiological
444 changes in the early postoperative period. 2) Both NP assessments as well as a WM
445 task were obtained. 3) It had a substantial scalp EEG coverage (62 channels instead
446 of 10 or 20 sensors). 4) The WM task featured a control condition to evaluate memory-
447 specific changes. 5) It examined an elderly cohort vulnerable to perioperative cognitive
448 changes. The study had the following limitations: 1) It was conducted at a prostate
449 cancer centre; thus, only men were included limiting generalisability of results. 2) There
450 was no matched control group, restricting our ability to differentiate session- from
451 purely anaesthesia-related changes. 3) Fifteen patients did not complete the second
452 session, potentially patients that suffered from more postoperative complications. High
453 drop-out rates are frequently reported in studies focusing on perioperative cognitive
454 disorders (Ref) and pose a relevant source of selection bias. To address this issue, we
455 compared demographic and clinical characteristics between patients, who completed
456 all pre- and postoperative assessments and those who did not without observing
457 relevant differences.

458

459 **Conclusion**

460 Here, we present empirical evidence that oscillatory and aperiodic dynamics
461 track different aspects of perioperative cognition. Specifically, aperiodic activity as an
462 index of population activity and anaesthesia-induced inhibition overhang might prove
463 to be a valuable biomarker in tracking cognitive function in the perioperative setting.

464

465

466 **Acknowledgments**

467 The authors would like to thank Randolph Helfrich, Hertie-Institute for Clinical Brain
468 Research, Tübingen, for his advice regarding data analysis as well as his valuable
469 input on the manuscript.

470

471 **Declaration of interests**

472 The authors declare that they have no conflict of interest.

473

474 **Funding**

475 This work was supported by a grant of the German Research Foundation (DFG LE
476 3863/2-1) to JDL.

477

478 **Details of author's contribution**

479 All authors declare that they took part in the revision of this manuscript, that they
480 approved of the final version and they agree to be accountable for all aspects of the
481 work. Furthermore, the authors contributed in the following areas: JDL: Data analysis,
482 data interpretation, writing of first draft of manuscript; UH: Patient recruitment, data
483 collection; JD, AKE, CZ: Study design; TS: Study design, data collection, data analysis
484 and interpretation; MF: Study design, patient recruitment, data collection, data analysis
485 and interpretation.

486

487 **Data and custom code availability**

488 Data will be made available upon reasonable request to Marlene Fischer
489 (mar.fischer@uke.de). Custom code will be shared upon reasonable request to the
490 corresponding author.

491 **References**

- 492 1. Guenther U, Radtke FM. Delirium in the postanaesthesia period. *Curr Opin*
493 *Anaesthesiol* 2011; **24**: 670–5
- 494 2. Radtke FM, Franck M, Lendner J, Krüger S, Wernecke KD, Spies CD.
495 Monitoring depth of anaesthesia in a randomized trial decreases the rate of
496 postoperative delirium but not postoperative cognitive dysfunction. *Br J Anaesth*
497 2013; **110 Suppl 1**: i98-105
- 498 3. Newman S, Stygall J, Hirani S, Shaefi S, Maze M. Postoperative cognitive
499 dysfunction after noncardiac surgery: a systematic review. *Anesthesiology* 2007; **106**:
500 572–90
- 501 4. Brown EN, Purdon PL. The aging brain and anesthesia. *Curr Opin*
502 *Anaesthesiol* 2013; **26**: 414–9
- 503 5. Koch S, Windmann V, Chakravarty S, et al. Perioperative
504 Electroencephalogram Spectral Dynamics Related to Postoperative Delirium in Older
505 Patients. *Anesth Analg* 2021; **133**: 1598–607
- 506 6. Steinmetz J, Christensen KB, Lund T, Lohse N, Rasmussen LS, ISPOCD
507 Group. Long-term consequences of postoperative cognitive dysfunction.
508 *Anesthesiology* 2009; **110**: 548–55
- 509 7. Phillips-Bute B, Mathew JP, Blumenthal JA, et al. Association of
510 neurocognitive function and quality of life 1 year after coronary artery bypass graft
511 (CABG) surgery. *Psychosom Med* 2006; **68**: 369–75
- 512 8. Messerotti Benvenuti S, Zanatta P, Longo C, Mazzarolo AP, Palomba D.
513 Preoperative cerebral hypoperfusion in the left, not in the right, hemisphere is
514 associated with cognitive decline after cardiac surgery. *Psychosom Med* 2012; **74**:
515 73–80
- 516 9. Tanino M, Kobayashi M, Sasaki T, et al. Isoflurane Induces Transient
517 Impairment of Retention of Spatial Working Memory in Rats. *Acta Med Okayama*
518 2016; **70**: 455–60
- 519 10. Tallon-Baudry C, Bertrand O, Peronnet F, Pernier J. Induced γ -Band Activity
520 during the Delay of a Visual Short-Term Memory Task in Humans. *J Neurosci*
521 Society for Neuroscience; 1998; **18**: 4244–54
- 522 11. Sarnthein J, Petsche H, Rappelsberger P, Shaw GL, von Stein A.
523 Synchronization between prefrontal and posterior association cortex during human
524 working memory. *Proc Natl Acad Sci U S A* 1998; **95**: 7092–6
- 525 12. Fell J, Axmacher N. The role of phase synchronization in memory processes.
526 *Nat Rev Neurosci* 2011; **12**: 105–18
- 527 13. Roux F, Uhlhaas PJ. Working memory and neural oscillations: alpha–gamma
528 versus theta–gamma codes for distinct WM information? *Trends in Cognitive*
529 *Sciences* 2014; **18**: 16–25
- 530 14. Donoghue T, Haller M, Peterson EJ, et al. Parameterizing neural power
531 spectra into periodic and aperiodic components. *Nat Neurosci* 2020; **23**: 1655–65
- 532 15. Lendner JD, Helfrich RF, Mander BA, et al. An electrophysiological marker of
533 arousal level in humans. Haegens S, editor. *eLife* eLife Sciences Publications, Ltd;
534 2020; **9**: e55092
- 535 16. Colombo MA, Napolitani M, Boly M, et al. The spectral exponent of the resting
536 EEG indexes the presence of consciousness during unresponsiveness induced by
537 propofol, xenon, and ketamine. *Neuroimage* 2019; **189**: 631–44
- 538 17. Gao R. Interpreting the electrophysiological power spectrum. *J Neurophysiol*

- 539 2016; **115**: 628–30
- 540 18. Waschke L, Donoghue T, Fiedler L, et al. Modality-specific tracking of
541 attention and sensory statistics in the human electrophysiological spectral exponent.
542 *Elife* 2021; **10**: e70068
- 543 19. Podvalny E, Noy N, Harel M, et al. A unifying principle underlying the
544 extracellular field potential spectral responses in the human cortex. *Journal of*
545 *Neurophysiology* American Physiological Society; 2015; **114**: 505–19
- 546 20. Daume J, Gruber T, Engel AK, Fries U. Phase-Amplitude Coupling and
547 Long-Range Phase Synchronization Reveal Frontotemporal Interactions during
548 Visual Working Memory. *J Neurosci* 2017; **37**: 313–22
- 549 21. Carbone E, Vianello E, Carretti B, Borella E. Working Memory Training for
550 Older Adults After Major Surgery: Benefits to Cognitive and Emotional Functioning.
551 *Am J Geriatr Psychiatry* 2019; **27**: 1219–27
- 552 22. Price CC, Garvan C, Hizek LP, Lopez MG, Billings FT. Delayed Recall and
553 Working Memory MMSE Domains Predict Delirium following Cardiac Surgery. *J*
554 *Alzheimers Dis* 2017; **59**: 1027–35
- 555 23. Zhang X, Jiang X, Huang L, et al. Central cholinergic system mediates
556 working memory deficit induced by anesthesia/surgery in adult mice. *Brain Behav*
557 2018; **8**: e00957
- 558 24. Snodgrass JG, Vanderwart M. A standardized set of 260 pictures: norms for
559 name agreement, image agreement, familiarity, and visual complexity. *J Exp Psychol*
560 *Hum Learn* 1980; **6**: 174–215
- 561 25. Oostenveld R, Fries P, Maris E, Schoffelen J-M. FieldTrip: Open source
562 software for advanced analysis of MEG, EEG, and invasive electrophysiological data.
563 *Comput Intell Neurosci* 2011; **2011**: 156869
- 564 26. Hipp JF, Siegel M. Dissociating neuronal gamma-band activity from cranial
565 and ocular muscle activity in EEG. *Front Hum Neurosci* 2013; **7**: 338
- 566 27. Engel AK, Fries P. Beta-band oscillations—signalling the status quo? *Current*
567 *Opinion in Neurobiology* 2010; **20**: 156–65
- 568 28. Miller EK, Lundqvist M, Bastos AM. Working Memory 2.0. *Neuron* 2018; **100**:
569 463–75
- 570 29. Spitzer B, Haegens S. Beyond the Status Quo: A Role for Beta Oscillations in
571 Endogenous Content (Re)Activation. *eNeuro* [Internet] Society for Neuroscience;
572 2017 [cited 2022 Feb 23]; **4** Available from:
573 <https://www.eneuro.org/content/4/4/ENEURO.0170-17.2017>
- 574 30. Staudigl T, Hanslmayr S. Theta oscillations at encoding mediate the context-
575 dependent nature of human episodic memory. *Curr Biol* 2013; **23**: 1101–6
- 576 31. Peterson EJ, Voytek B. Alpha oscillations control cortical gain by modulating
577 excitatory-inhibitory background activity [Internet]. 2017 Sep p. 185074 Available
578 from: <https://www.biorxiv.org/content/10.1101/185074v2>
- 579 32. Jensen O, Bonnefond M, Marshall TR, Tiesinga P. Oscillatory mechanisms of
580 feedforward and feedback visual processing. *Trends in Neurosciences* 2015; **38**:
581 192–4
- 582 33. Jensen O, Mazaheri A. Shaping Functional Architecture by Oscillatory Alpha
583 Activity: Gating by Inhibition. *Front Hum Neurosci* 2010; **4**: 186
- 584 34. Lundqvist M, Rose J, Herman P, Brincat SL, Buschman TJ, Miller EK. Gamma
585 and Beta Bursts Underlie Working Memory. *Neuron* 2016; **90**: 152–64
- 586 35. Park H-D, Min B-K, Lee K-M. EEG oscillations reflect visual short-term
587 memory processes for the change detection in human faces. *Neuroimage* 2010; **53**:

- 588 629–37
- 589 36. Fries P. Rhythms For Cognition: Communication Through Coherence. *Neuron*
590 2015; **88**: 220–35
- 591 37. Labonte AK, Kafashan M, Huels ER, et al. The posterior dominant rhythm: an
592 electroencephalographic biomarker for cognitive recovery after general anaesthesia.
593 *British Journal of Anaesthesia* [Internet] Elsevier; 2022 [cited 2022 Feb 22]; **0**
594 Available from: [https://www.bjanaesthesia.org.uk/article/S0007-0912\(22\)00028-](https://www.bjanaesthesia.org.uk/article/S0007-0912(22)00028-9/fulltext)
595 [9/fulltext](https://www.bjanaesthesia.org.uk/article/S0007-0912(22)00028-9/fulltext)
- 596 38. Miller KJ, Zanos S, Fetz EE, den Nijs M, Ojemann JG. Decoupling the cortical
597 power spectrum reveals real-time representation of individual finger movements in
598 humans. *J Neurosci* 2009; **29**: 3132–7
- 599 39. Voytek B, Kramer MA, Case J, et al. Age-Related Changes in 1/f Neural
600 Electrophysiological Noise. *J Neurosci* 2015; **35**: 13257–65
- 601 40. Mashour GA, Palanca BJ, Basner M, et al. Recovery of consciousness and
602 cognition after general anesthesia in humans. O’Connell RG, Ivry RB, O’Connell RG,
603 Tristan B, editors. *eLife* eLife Sciences Publications, Ltd; 2021; **10**: e59525
- 604 41. Brown EN, Lydic R, Schiff ND. General anesthesia, sleep, and coma. *N Engl J*
605 *Med* 2010; **363**: 2638–50
- 606 42. Evered LA, Chan MTV, Han R, et al. Anaesthetic depth and delirium after
607 major surgery: a randomised clinical trial. *Br J Anaesth* 2021; **127**: 704–12
- 608 43. Fritz BA, Maybrier HR, Avidan MS. Intraoperative electroencephalogram
609 suppression at lower volatile anaesthetic concentrations predicts postoperative
610 delirium occurring in the intensive care unit. *British Journal of Anaesthesia* Elsevier;
611 2018; **121**: 241–8
- 612 44. Pedemonte JC, Plummer GS, Chamadia S, et al. Electroencephalogram
613 Burst-suppression during Cardiopulmonary Bypass in Elderly Patients Mediates
614 Postoperative Delirium. *Anesthesiology* 2020; **133**: 280–92
- 615

616 **Tables**

617 **Table 1**

	N = 26
Age (y)	66 ± 3
Body Mass Index (kg/m²)	27.6 ± 3.5
Obesity	6 (23.1)
Hypertension	17 (65.4)
Coronary artery disease	3 (11.5)
Diabetes	1 (3.8)
Dyslipoproteinaemia	8 (30.8)
Smoking	4 (15.4)
ASA Physical Status	
<i>I</i>	2 (7.7)
<i>II</i>	24 (92.3)
<i>III</i>	0 (0.0)
Midazolam	
<i>Yes</i>	13 (50.0)
<i>No</i>	13 (50.0)
Sufentanil (µg)	104.0 ± 23.3
Infused Volume (ml)	2981 ± 640
Cristalloids (ml)	2865 ± 540
Colloids (ml)	
Blood Loss (ml)	408 ± 315
Surgery Duration (min)	225 ± 50
Anaesthesia Duration (min)	275 ± 54
PACU Length of stay (min)	178 ± 62

618

619

620 **Demographic and clinical characteristics of patients with complete pre- and postoperative**
621 **assessments (N = 26).** ASA – American Society of Anesthesiology Status (1 – no comorbidities, 2 –
622 mild systemic disease such as hypertension or diabetes). Data are given as mean ± SD or n (%).

622

623

624

625 **Table 2**

	Se 1				Se 2			
	Mem	Ctrl	Match	Non-Match	Mem	Ctrl	Match	Non-Match
Reaction Times (s)	1.104 ± 0.042	1.156 ± 0.081	1.131 ± 0.045	1.076 ± 0.044	1.119 ± 0.032	1.1484 ± 0.069	1.129 ± 0.037	1.109 ± 0.030
Accuracy	0.778 ± 0.011	0.7988 ± 0.014	0.791 ± 0.023	0.766 ± 0.022	0.786 ± 0.012	0.794 ± 0.012	0.835 ± 0.022	0.737 ± 0.022
Slope	-0.272 ± 0.083				-0.129 ± 0.098			
D-prime	1.658 ± 0.074				1.758 ± 0.103			
Bias	-0.065 ± 0.074				-0.213 ± 0.069			

626
627
628
629

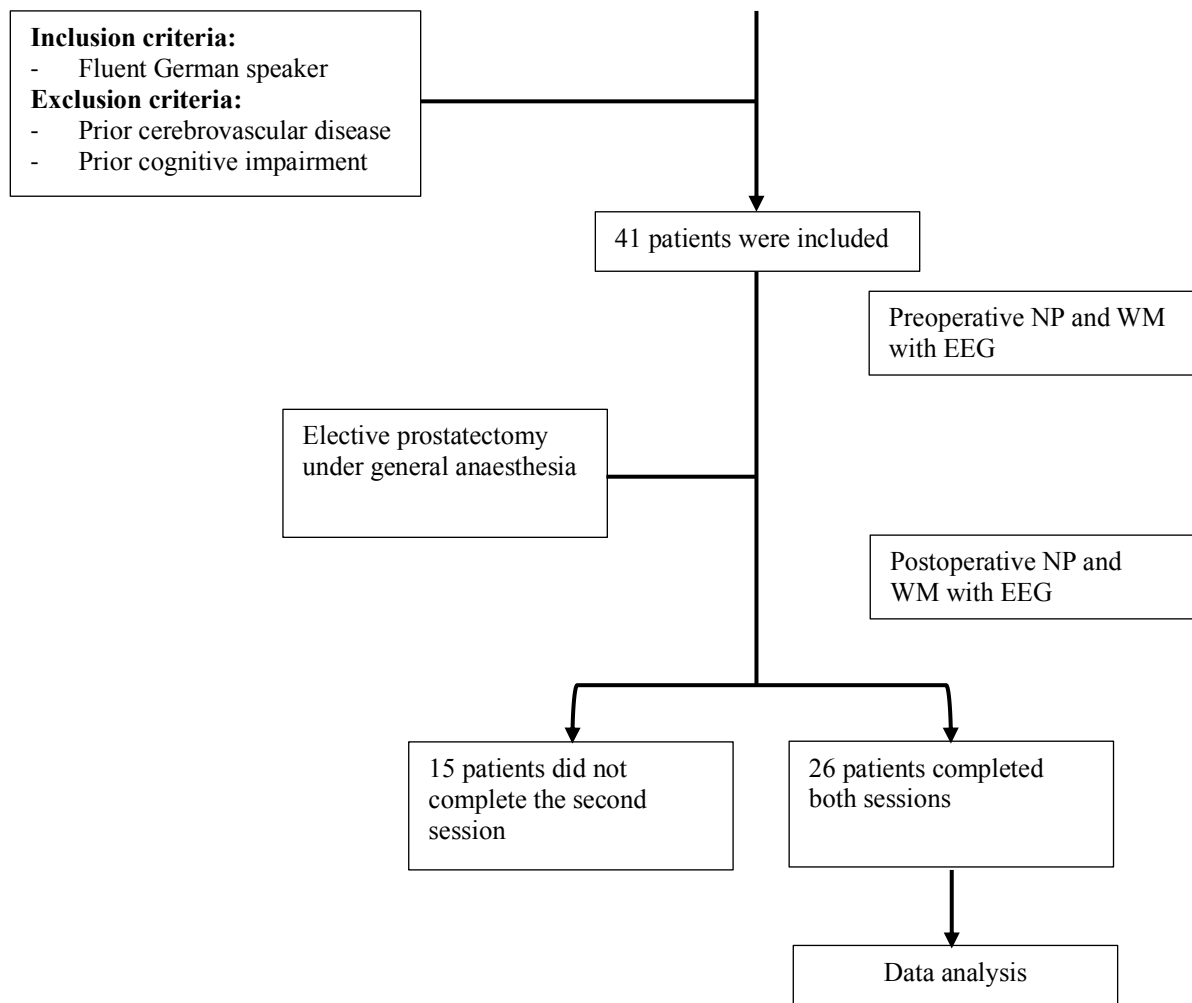
Working memory performance (n = 26). All values mean ± SEM. Se – session. Mem – memory, Ctrl – control condition.

630 **Supplemental Information**

631

632 **Supplemental Material and Methods**

633 *Flow Diagram of Study*



634 **Fig. S1: Flow Chart**

635

636 *Working Memory Task*

637 Each trial of both memory and control condition began with a fixation dot,
638 followed by a 200 ms sample presentation and a 3000 ms delay period in which the
639 fixation dot reappeared. In the memory condition, patients were then presented with

640 the probe for 200 ms (**Fig. 1**) and had to indicate whether the probe matched the
641 sample (match) or not (non-match). Responses were registered by pressing one of two
642 buttons using either their index or middle finger (counterbalanced). The inter-trial
643 interval was randomly jittered in steps of 100 ms ranging from 2.5 to 3 seconds. In the
644 control condition, an ellipse was presented for 50 ms instead of a second image. Here,
645 patients had to report whether the ellipse was vertically or horizontally oriented.¹⁵
646 Performance in the control condition was matched to the memory condition by
647 changing the shape and luminance of the ellipse.¹⁵ In addition, in 20% of control trials,
648 the contrast and shape were chosen randomly to disguise the relationship to memory
649 performance.¹⁵ Before the beginning of the recording, patients had a training session
650 where 4 trials of each condition were presented that were not part of the consecutive
651 task.¹⁵

652

653 *Anaesthesiologic management*

654 General anaesthesia was induced with sufentanil (0.3–0.7 µg/kg) and propofol
655 (2–3 mg/kg) followed by neuromuscular blockade with rocuronium (0.6 mg/kg) to
656 facilitate endotracheal intubation. A gastric tube was inserted in all patients and
657 prophylactic antiemetic medication was administered preoperatively (dexamethasone
658 4 mg). During surgery, rocuronium was titrated under the guidance of neuromuscular
659 blockade monitoring (train-of-four, TOF-Watch Organon; IntelliVue NMT module,
660 Philips GmbH, Hamburg, Germany). Anaesthesia depth was monitored with a
661 bispectral index monitor (BIS™, Medtronic GmbH, Meerbusch, Germany).
662 Sevoflurane-sufentanil was used for anaesthesia maintenance to achieve an end-tidal
663 sevoflurane concentration of 2.0 vol% (MAC 0.8–1.2). To maintain normothermia we
664 used a forced-air warming system throughout the entire procedure. Patients who

665 underwent robot-assisted surgery received peritoneal insufflation with carbon dioxide
666 and were positioned at a 45-degree head-down tilt. Postoperative pain management
667 included non-opioid medication (metamizole 1000 mg/100 ml) 30 minutes before
668 emergence and every 4–6 hours thereafter. In the post-anaesthesia care unit (PACU)
669 piritramide 3.75–7.5 mg was administered intravenously when pain scores exceeded
670 3. Subsequent PACU management in all patients included frequent control of wound
671 drains and postoperative urine output, blood gas analyses, and pain management as
672 described above.

673

674 *Data cleaning – Excluded channels and trials*

675 In total, 56 channels of Session 1 (not including EOG leads; 3.47 %) and 68
676 channels for Session 2 (4.29 %) were excluded, averaging to 2.15 channels/subject
677 in Session 1 and 2.62 channels/subject in Session 2. Excluded channels were
678 interpolated using their neighbours (ft_channelrepair). Regarding trials, a total of 194
679 trials of Session 1 (3.59 %) and 172 trials of Session 2 (3.18 %) were identified as
680 noisy and removed, averaging to 7.46 trials/subject for Session 1 and 6.62
681 trials/subject for Session 2.

682

683 *Event-Related Potential (ERP) analysis*

684 For ERP analysis, electrophysiological data of each session was low-pass
685 filtered below 30 Hz and split into memory and control conditions. Data was then time-
686 locked to the respective baseline (-200 - 0 ms before sample presentation) and
687 averaged across trials. For a comparison between conditions, we averaged across
688 sessions (**Fig. S5**).

689

690

691 *Beamformer analysis*

692 We source-localized power differences in frequency bands of interest and their
693 significant correlation with WM performance (Fig. 3, 4). Cortical sources of the sensor-
694 level EEG data were reconstructed by using a LCMV (linearly constraint minimum
695 variance) beamforming approach²⁰ to estimate the time series for every voxel on the
696 grid. A standard T1 MRI template and a BEM (boundary element method) headmodel
697 from the FieldTrip toolbox¹⁹ were used to construct a 3D template grid at 1cm spacing
698 in standard MNI space. Electrode location were positioned on a standard head and
699 aligned with MNI space using the FieldTrip toolbox¹⁹. Prior to source projection, sensor
700 level data was common average referenced and epoched into 5 second segments. To
701 minimize computational load, we selected a two second data segment (1 to 3 seconds)
702 from the delay period of every epoch to construct the covariance matrix. The LCMV
703 spatial filter was then calculated using the covariance matrix of the sensor-level EEG
704 data with 5% regularization. Spatial filters were constructed for each of the grid
705 positions separately to maximally suppress activity from all other sources. The
706 resulting time courses in source space then underwent spectral analysis using a
707 Fourier transform using a multitaper approach (*'mtmfft'* of *ft_freqanalysis* from FieldTrip
708 using *'dpss'* taper, a smoothing frequency +/- 1 Hz and a 0,5 second moving time
709 window). For the memory/control comparison, power spectra were averaged across
710 sessions prior to statistical analysis. Power differences between both memory and
711 control and well as between memory sessions, and their correlation with behaviour
712 were then tested using cluster-based permutation approaches employing either
713 repeated t-tests or correlation (see below for details). The results were calculated at

714 every voxel in source space, converted to z-values and then interpolated onto a
 715 standard template brain in MNI space.

716 **Supplemental Results**

717

718 *Patient characteristics*

719

720 **Table S1**

	Pre- and postoperative assessments completed (n=26)	Incomplete assessments (n=15)
Age (y)	66 ± 3	69 ± 4
Body Mass Index (kg/m²)	27.6 ± 3.5	26.7 ± 3.2
Obesity	6 (23.1)	3 (20.0)
Hypertension	17 (65.4)	6 (40.0)
Coronary artery disease	3 (11.5)	1 (6.7)
Diabetes	1 (3.8)	2 (13.3)
Dyslipoproteineamia	8 (30.8)	2 (13.3)
Smoking	4 (15.4)	0 (0.0)
ASA Status		
<i>I</i>	2 (7.7)	0 (0.0)
<i>II</i>	24 (92.3)	13 (86.7)
<i>III</i>	0 (0.0)	2 (13.3)
Midazolam		
<i>Yes</i>	13 (50.0)	7 (46.7)
<i>No</i>	13 (50.0)	8 (53.3)
Sufentanil (µg)	104.0 ± 23.3	98.2 ± 18.3
Infused Volume (ml)	2981 ± 640	2767 ± 704
Cristalloids (ml)	2865 ± 540	2767 ± 704
Colloids (ml)		
Blood Loss (ml)	408 ± 315	503 ± 303
Surgery Duration (min)	225 ± 50	206 ± 49
Anaesthesia Duration (min)	275 ± 54	261 ± 61
PACU Length of Stay (min)	178 ± 62	183 ± 53

721

722 **Characteristics of patients with complete (n=26) and incomplete pre- and postoperative**
 723 **assessments (n = 15).** ASA – American Society of Anesthesiology Status (1 – no comorbidities, 2 –
 724 mild systemic disease such as hypertension or diabetes). SD – standard deviation. Data are presented
 725 as mean ± SD or n (%).

726

727

728 *Behavioural Performance – Neuropsychological Assessment*

729

730 **Table S2**

	Se 1		Se 2		z-score	
	Mean	SD	Mean	SD	Mean	SD
Total recall	44	9	40	9	-0.42	0.66
Learning slope	1	0	1	0	-0.31	0.81
TMT_B (s)	80	22	73	20	-0.17	0.54
GPT_dom (s)	82	8	80	11	-0.08	.055
Digit Span	5	1	5	1	-0.04	0.79

731

732 **Absolute values and z-scores of neuropsychological assessments (n = 26).** Se – session. TMT –
733 Trail Making Test. GPT – Grooved-Pegboard Test. dom – dominant. Data are presented as mean ± SD.

734

735 *Behavioural Performance – Working Memory Reaction times*

736 In the WM task, there was no significant influence of condition or session on
737 reaction times (RT; *repeated-measures ANOVA*: condition $F_{1,25} = 0.366$, $p = 0.551$;
738 session $F_{1,25} = 0.008$, $p = 0.928$; condition*session $F_{1,25} = 0.216$, $p = 0.646$; **Table 2**).
739 However, patients exhibited a tendency to be faster for the non-match than the match
740 trials (see **Table S2**; *repeated-measures ANOVA*: match $F_{1,25} = 3.785$, $p = 0.063$;
741 session $F_{1,25} = 0.141$, $p = 0.710$; match*session $F_{1,25} = 0.929$, $p = 0.344$).

742

743 *Event-related potentials differentiate memory and control conditions*

744 We could identify a total two clusters that marked significant differences on the
745 group level: One late (*cluster-based permutation t-tests*: 1 to 3.1 s, $t_1 = -8.87 \cdot 10^4$, $p_1 =$
746 0.002 , 37 channels with a focus on posterior parietal cortex) and one early in the delay
747 period (reflecting the p300; 0.2 to 1 s, $t_2 = -4.74 \cdot 10^4$, $p_2 = 0.004$, 34 CH posterior
748 parietal) mirrored by two positive ones (early 0.2 to 1 s, $p_1 = 0.014$, $t_1 = 4.06 \cdot 10^4$, 43
749 channels over frontal cortex; late 2.1 to 2.95 s, $p_2 = 0.016$, $t_2 = 3.27 \cdot 10^4$, 22 frontal
750 channels; see **Fig. S5**).

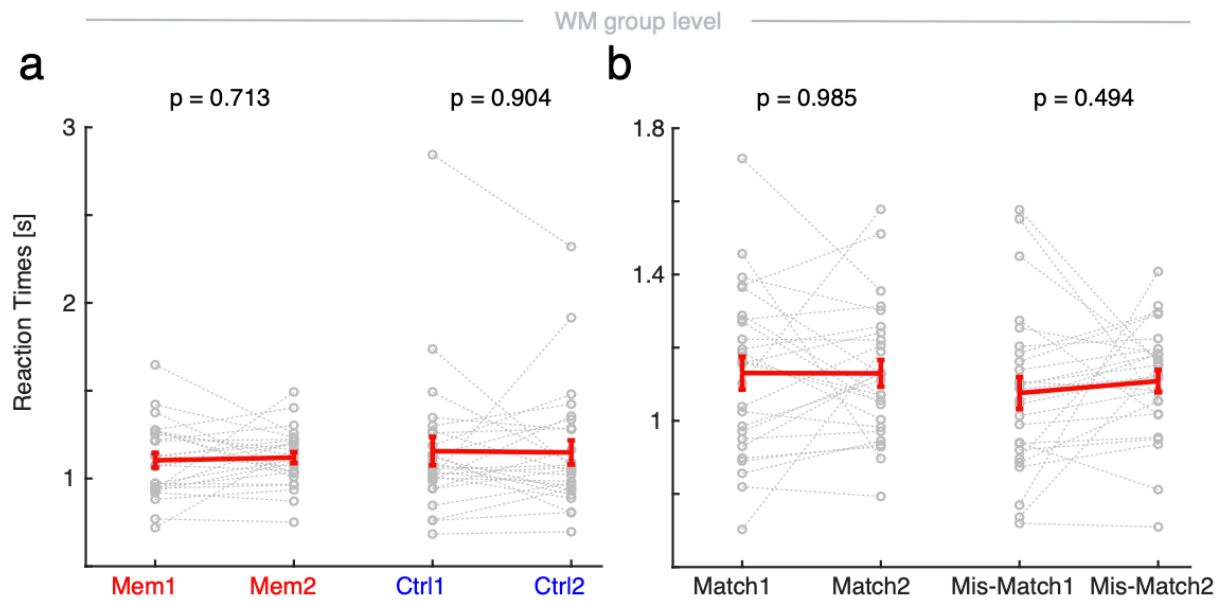
751 When contrasting the ERPs of the post- and pre-anaesthesia memory sessions
752 (Se2-Se1), there were no significant differences (*cluster-based permutation t-tests*:
753 one positive cluster of 11 central channels, 0.57 to 0.9 s, $p = 0.272$, $t = 5.14 \cdot 10^4$). Note,
754 that both the comparison of ERPs of control sessions or the memory-control
755 differences did not show significant differences as well (Ctrl: positive cluster. 10 central
756 channels, $p = 0.296$, $t = 4.68 \cdot 10^3$; Difference: positive cluster, 15 central channels, p
757 $= 0.805$, $t = 2.31 \cdot 10^3$; **Fig. S5**).

758

759 **Supplemental Figures**

760

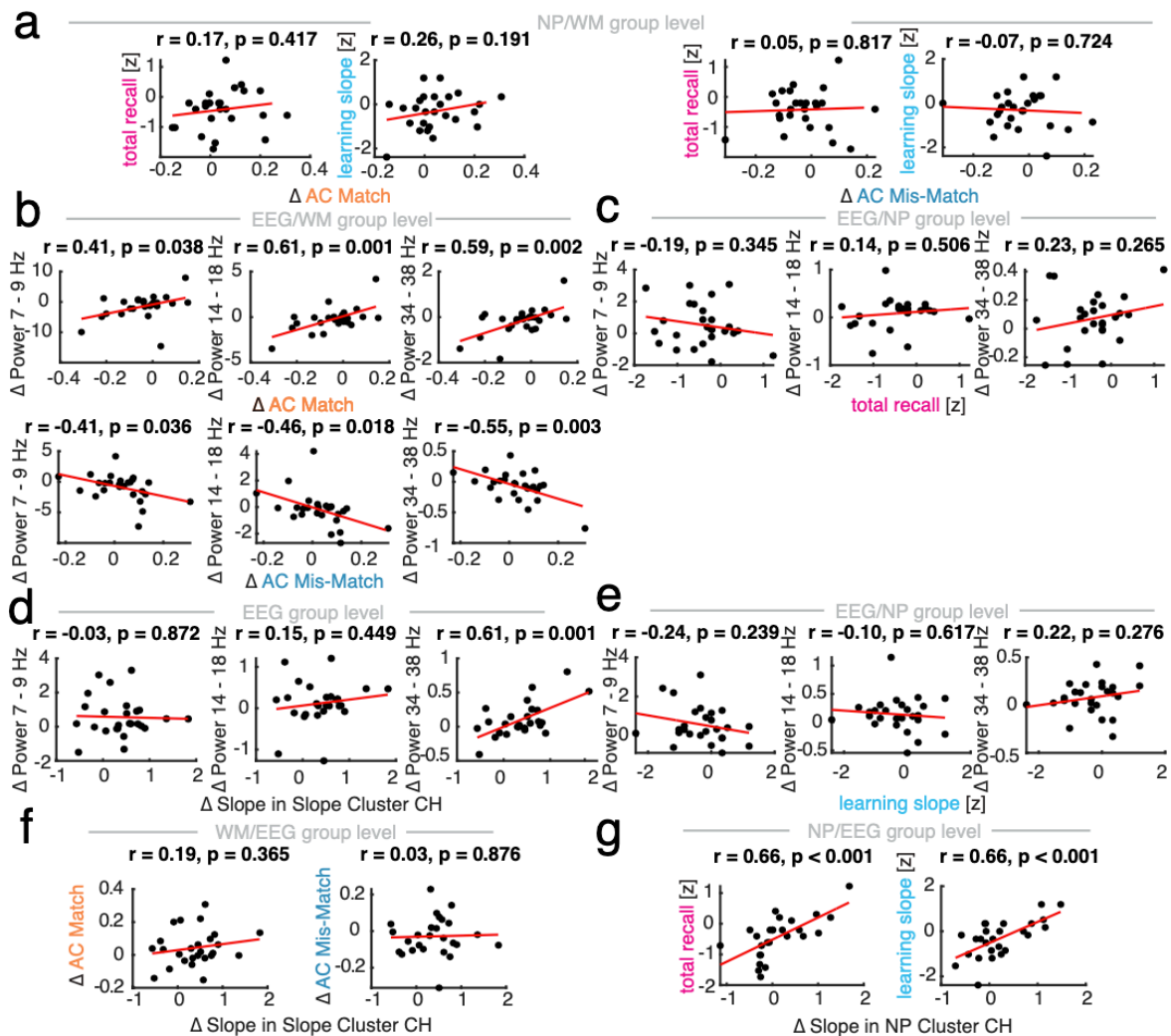
761



762

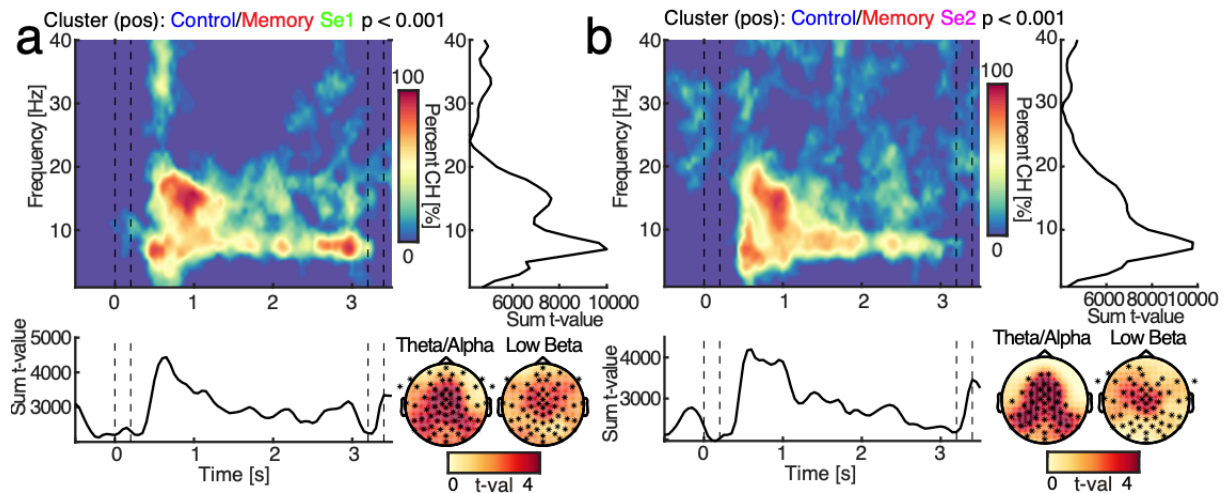
763 **Figure S2: Behaviour in the visual working memory task.**

764 **a**, Reaction times in seconds (s) in memory and control condition before (1) and after (2) anaesthesia
765 (n = 26). *Repeated-measures ANOVA*: condition $F_{1,25} = 0.366$, $p = 0.551$; session $F_{1,25} = 0.008$, $p =$
766 0.928 ; condition*session $F_{1,25} = 0.216$, $p = 0.646$. Grey dots – single subjects. Red line – mean ± SEM.
767 P-values *post-hoc uncorrected t-tests*. **b**, Reaction times in seconds (s) between memory sessions in
768 match and non-match trials. *Repeated-measures ANOVA*: match $F_{1,25} = 3.785$, $p = 0.063$; session $F_{1,25}$
769 $= 0.141$, $p = 0.710$; match*session $F_{1,25} = 0.929$, $p = 0.344$. Grey dots – single subjects. Red line – mean
770 ± SEM. P-values *post-hoc uncorrected t-tests*.
771



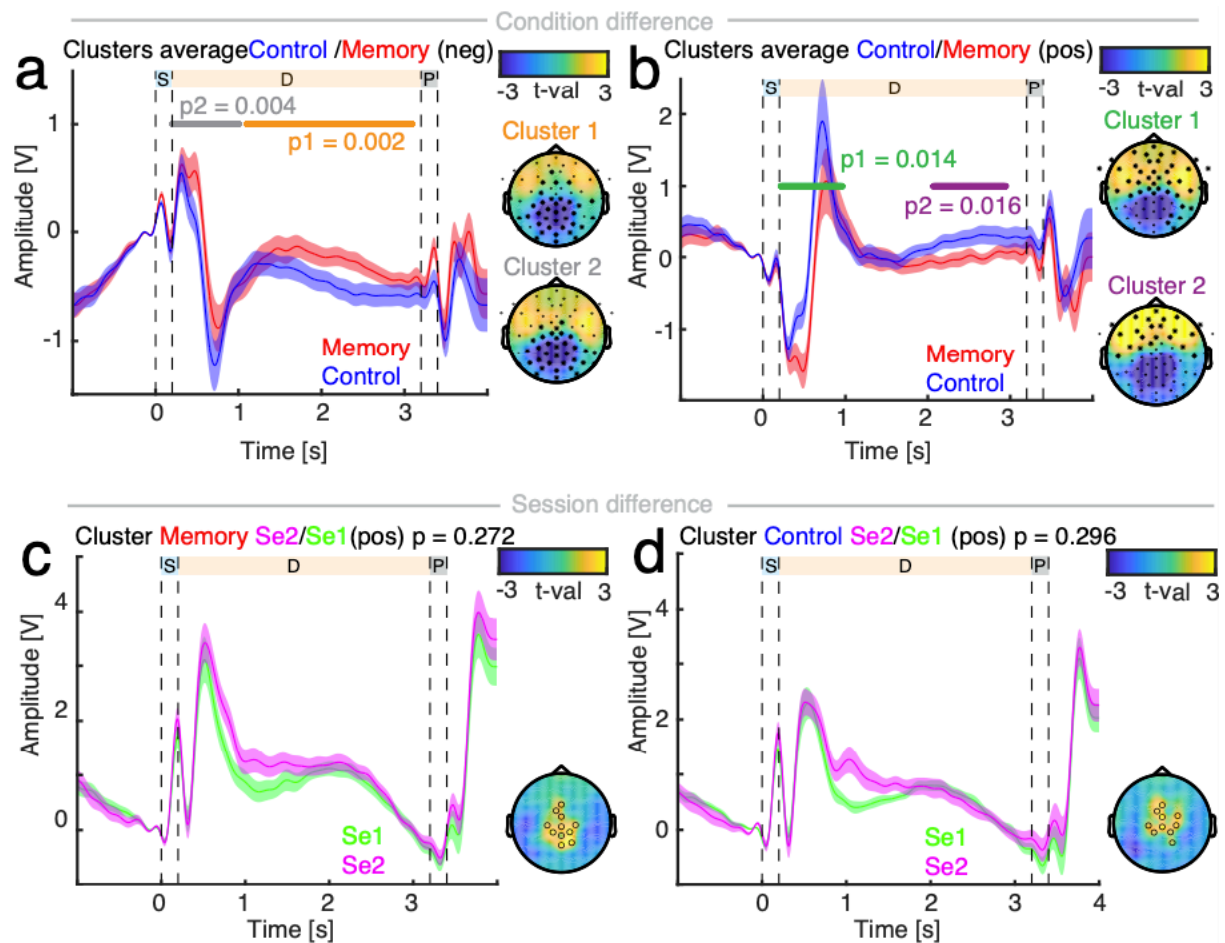
772
773
774
775
776
777
778
779
780
781
782
783
784
785
786
787
788
789
790
791
792
793
794

Figure S3: Associations between neuropsychological assessment, working memory performance, oscillatory and aperiodic electrophysiological features. **a**, Association of neuropsychological (NP) assessment (z-scores of California Verbal Learning Task (CVLT) total recall and learning slope) and session differences in performance between the memory sessions of the working memory (WM) task (Δ Se2-Se1, $n = 26$). Left – total recall and learning slope with Δ match accuracy; Right – Δ mis-match accuracy. **b**, Association of electroencephalogram (EEG) oscillatory power differences between memory sessions in frequency bands of interest (Δ Se2-Se1, $n = 26$) and WM Δ match and Δ mis-match accuracy in cluster channels (*post-hoc correlations*; session differences in spectral power and accuracy *cluster-permutation test*: Δ AC match $p < 0.01$, Δ AC mis-match $p = 0.022$; **Fig. 4**). **c**, Association of EEG oscillatory power differences between memory sessions in frequency bands of interest (Δ Se2-Se1, $n = 26$) and NP z-score of CVLT total recall. **d**, Association of EEG oscillatory power differences between memory sessions in frequency bands of interest (Δ Se2-Se1, $n = 26$) and EEG spectral slope (30 – 40 Hz) difference between memory sessions in cluster channels (Δ Se2-Se1 spectral slope *cluster-permutation test*: $p = 0.073$, **Fig. 5**). **e**, Association of EEG oscillatory power differences between memory sessions in frequency bands of interest (Δ Se2-Se1, $n = 26$) and NP z-score of CVLT learning slope (**Fig. 5**). **f**, Association between WM performance and EEG Δ spectral slope (Δ Se2-Se1, $n = 26$). Left – accuracy in match and Right – accuracy in mis-match discrimination in slope difference cluster channels. **g**, Association between NP performance and EEG Δ spectral slope (Δ Se2-Se1, $n = 26$). Left – z-score CVLT total recall and Right – z-score CVLT learning slope in NP cluster channels (Δ spectral slope and total recall *cluster-permutation test*: $p = 0.029$; Δ spectral slope and learning slope *cluster-permutation test*: $p = 0.015$; **Fig. 5**).



795
796
797
798
799
800
801
802
803
804
805
806
807
808
809
810
811
812
813
814

Figure S4: Spectral power changes in pre- and post-anaesthesia session. Sequence of WM task: blue/S – sample presentation, orange/D – delay, grey/P – probe presentation.
a, Control and memory condition power differences (baseline-corrected) in the pre-anaesthesia session (Se1). Left upper panel – Spectral power changes between control and memory in session 1 ($p < 0.001$, $n = 26$). Colour-coded is the number of channels that are part of the cluster from blue – no channels to red – 100% of channels. Right upper panel – Sum of t-values per frequency. Note the peaks in the theta/alpha (7 – 9 Hz) and low beta (14 – 18 Hz) frequency range. Left middle panel – Sum of t-values per time. Note the increased activity in the theta/alpha band in the control condition, revealing a sustained suppression in the memory session. Right middle panel – spatial extent of spectral power difference between conditions in the theta/alpha and low beta band.
b, Post-(Se2) anaesthesia control and memory condition power differences (baseline-corrected). Left upper panel – Spectral power changes between control and memory in session 2 ($p < 0.001$, $n = 26$). Colour-coded is the number of channels that are part of the cluster from blue – no channels to red – 100% of channels. Right upper panel – Sum of t-values per frequency. Note the peaks in the that/alpha (7-9 Hz) and low beta (14 – 18 Hz) frequency range. Left middle panel – Sum of t-values per time. Right middle panel – spatial extent of condition difference in the theta/alpha (7-9 Hz) and low beta frequency (14 – 18 Hz).



815

816 **Figure S5: Comparison of condition and session Event-related potentials.**

817 Sequence of WM task: blue/S – sample, orange/D – delay, grey/P – probe.

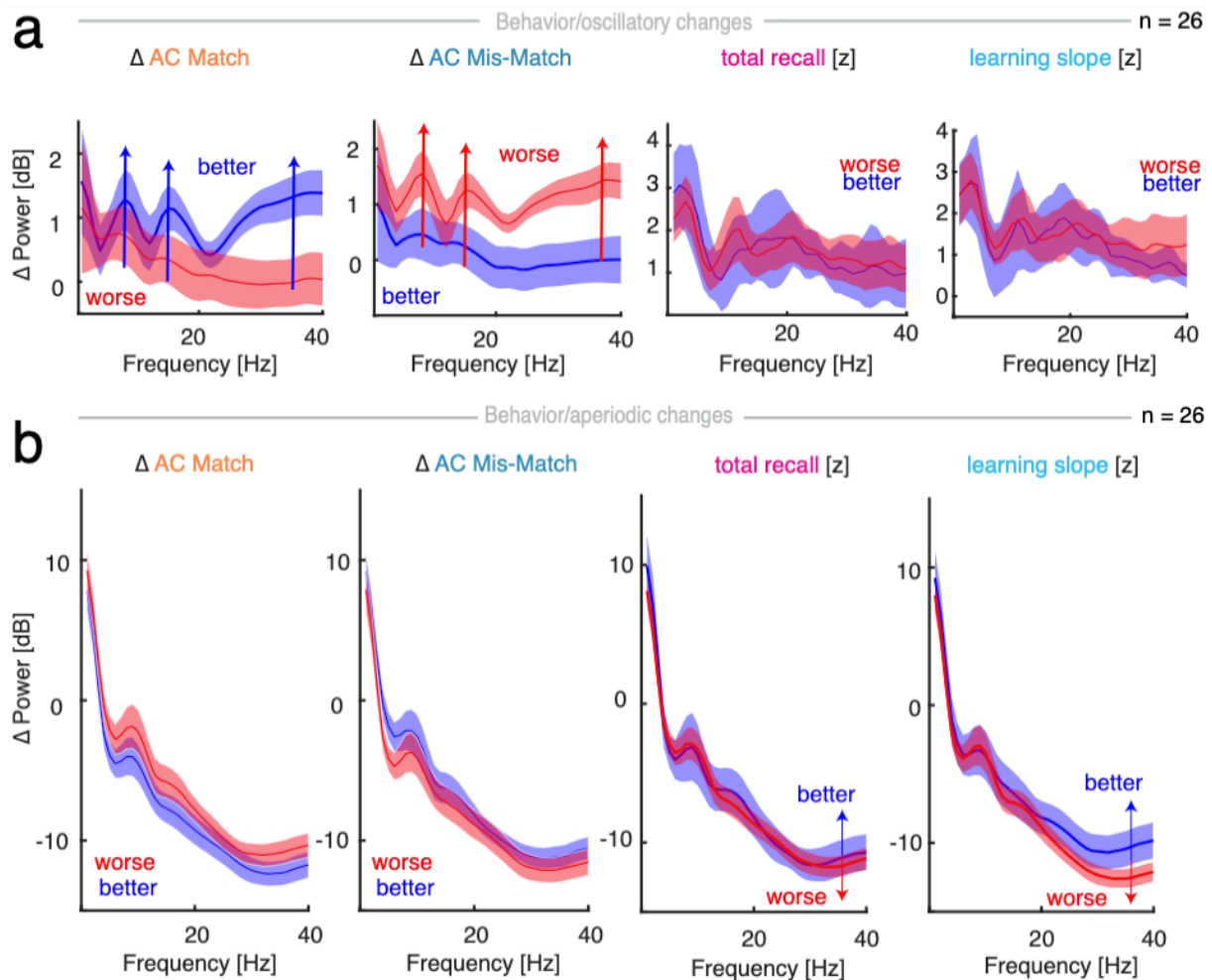
818 **a**, Temporal (left) and spatial (right) extent of condition differences of event-related potentials (ERP)
 819 between average control (blue) and memory (red; $n = 26$). Two negative, parieto-central clusters were
 820 significant: First one in delay (orange, $p = 0.002$), second one early (grey, $p = 0.004$) reflecting the ERP.

821 **b**, Temporal (left) and spatial (right) extent of ERP differences between average memory (red) and
 822 control (blue). Two positive frontal clusters emerged: First one early (green, $p = 0.014$) reflecting the
 823 ERP, second late in delay (purple, $p = 0.016$). Note the mirrored effect compared to a.

824 **c**, Pre- (green) and post-anaesthesia (magenta) memory sessions did not show significant temporal
 825 (left) or spatial (right) ERP differences.

826 **d**, Pre- (green) and post-anaesthesia (magenta) control sessions did not show significant temporal (left)
 827 or spatial (right) ERP differences.

828



829
830
831
832
833
834
835
836
837
838
839
840
841
842
843
844
845
846
847

Figure S6: Electrophysiological signatures by median split of cognitive performances.

a, Oscillatory changes: median split of baseline-corrected spectral power differences between post- and pre-anaesthesia sessions (Δ Se2 - Se1, n = 26). Left – split by median difference (Δ Se1-Se2) of Δ accuracy of match discrimination; left middle - Δ mis-match discrimination. Note, the power differences in certain frequency bands (theta, low and high beta). Right middle – Power split by median z-score of neuropsychological assessment by the California Verbal Learning Task (CVLT) total recall and right – learning slope. Blue – better performance than median, red – worse performance than median. Note, that there are no relevant oscillatory changes that track NP performance.

b, Aperiodic changes: median split of spectral power differences between post- and pre-anaesthesia memory sessions (Δ Se2 - Se1, n = 26). Left – Power split by median difference (Δ Se1-Se2) of accuracy of match; left middle – mis-match discrimination. Right middle – Power split by median z-score of neuropsychological assessment by CVLT total recall and right – learning slope. Note, the diverging steepness of the power spectrum above 30 Hz compared to the accuracy difference splits. Blue – better performance than median, red – worse performance than median.